Development 134, 31-41 (2007) doi:10.1242/dev.02722

Gene replacement reveals a specific role for E-cadherin in the formation of a functional trophectoderm

Natalia G. Kan[1,*], Marc P. Stemmler[1], Dirk Junghans[1], Benoît Kanzler[1], Wilhelmine N. de Vries[2], Mara Dominis[3] and Rolf Kemler[1,†]

During mammalian embryogenesis the trophectoderm represents the first epithelial structure formed. The cell adhesion molecule E-cadherin is ultimately necessary for the transition from compacted morula to the formation of the blastocyst to ensure correct establishment of adhesion junctions in the trophectoderm. Here, we analyzed to what extent E-cadherin confers unique adhesion and signaling properties in trophectoderm formation in vivo. Using a gene replacement approach, we introduced N-cadherin cDNA into the E-cadherin genomic locus. We show that the expression of N-cadherin driven from the E-cadherin locus reflects the expression pattern of endogenous E-cadherin. Heterozygous mice co-expressing E- and N-cadherin are vital and show normal embryonic development. Interestingly, N-cadherin homozygous mutant embryos phenocopy E-cadherin-null mutant embryos. Upon removal of the maternal E-cadherin, we demonstrate that N-cadherin is able to provide sufficient cellular adhesion to mediate morula compaction, but is insufficient for the subsequent formation of a fully polarized functional trophectoderm. When ES cells were isolated from N-cadherin homozygous mutant embryos and teratomas were produced, these ES cells differentiated into a large variety of tissue-like structures. Importantly, different epithelial-like structures expressing N-cadherin were formed, including respiratory epithelia, squamous epithelia with signs of keratinization and secretory epithelia with goblet cells. Thus, N-cadherin can maintain epithelia in differentiating ES cells, but not during the formation of the trophectoderm. Our results point to a specific and unique function for E-cadherin during mouse preimplantation development.

KEY WORDS: E-cadherin, N-cadherin, Trophectoderm formation, Cell adhesion, Gene replacement, Mouse

INTRODUCTION

The programmed development of a fertilized egg into a highly organized organism is ultimately dependent on cell-cell interactions mediated by cellular adhesion molecules. These include the classical cadherins, such as E- and N-cadherin, which are calcium-dependent cell adhesion molecules that exhibit unique and mostly mutually exclusive spatio-temporal expression patterns often associated with important morphogenetic processes (Gumbiner, 2005; Takeichi, 1988). E-cadherin [E-cad; cadherin 1 (Cdh1) – Mouse Genome Informatics] was found to be a key molecule for preimplantation development, and it is already present in the unfertilized egg as maternal mRNA and protein (Kemler et al., 1977; Ohsugi et al., 1997). Specifically, E-cad is vital for the compaction process at morula stage and the ensuing formation of trophectoderm, the first polarized epithelial cell layer in the mouse embryo. At gastrulation, E-cad is downregulated in the emerging mesoderm, where N-cadherin [N-cad; cadherin 2 (Cdh2) – Mouse Genome Informatics] becomes expressed (Butz and Larue, 1995; Takeichi, 1988). Similarly, during neurulation, an E- to N-cad switch takes place in the neural plate as it invaginates (Hatta and Takeichi, 1986). In contrast to the expression of E-cad, which is largely confined to epithelia, N-cad expression is restricted to neural tissues, the notochord and cells of mesenchymal origin such as somites and cardiac and skeletal muscles (Hatta and Takeichi, 1986; Radice et al., 1997). Opposing roles of E- and N-cad are also observed during tumor formation and in the invasiveness of metastatic cells (Hazan et al., 2004; Li and Herlyn, 2000; Tomita et al., 2000). In tumors of epithelial origin, E-cad acts as an invasion suppressor, and loss of E-cad expression correlates with tumor progression and malignancy in mouse and humans (Christofori and Semb, 1999; Nollet et al., 1999). Although N-cad is generally not expressed in normal epithelial cells, it is upregulated in many cancer cell lines and tumors and N-cad expression correlates with invasiveness, increased motility and the metastatic potential of cancer cells (Hazan et al., 2000; Islam et al., 1996; Suyama et al., 2002).

E- and N-cad share several structural and functional features. Both are single-span transmembrane glycoproteins with an extracellular region, a transmembrane helix and a cytoplasmic domain (Gumbiner, 1996; Kemler, 1993). The extracellular region has a modular structure composed of five cadherin-binding domains that are separated from each other by Ca^{2+}-binding pockets. The cytoplasmic domain serves as a scaffold for intracellular binding partners, such as catenins, that link cadherins to the cytoskeleton (Nose et al., 1990; Ozawa et al., 1989). Both E- and N-cad are calcium-dependent cell adhesion molecules and undergo homophilic interactions (Nose et al., 1990; Shapiro et al., 1995). Heterophilic interactions with other adhesion molecules have also been described, but these usually confer low adhesiveness (Cepek et al., 1994; Corps et al., 2001). E-cad and N-cad first form cis-dimers on the cell surface, followed by homophilic trans-interaction with molecules on neighboring cells (Koch et al., 2004). This results in a local enrichment and clustering of these adhesion molecules, which is believed to be the basis for the strong adhesive state of cadherins typically seen in adherens junctions (Kemler, 1993). Different experimental approaches have helped to unravel the molecular basis of cadherin-mediated adhesion (Baumgartner et al., 2000; Duguay et al., 2003; Niessen and Gumbiner, 2002; Perret et al., 2002; Sivasankar et al., 2001). Using a quantitative dual pipette assay, the

[1]Max-Planck-Institut für Immunbiologie, Abteilung für Molekulare Embryologie, Stübeweg 51, D-79108 Freiburg, Germany. [2]The Jackson Laboratory, Bar Harbor, ME 04609-1500, USA. [3]Department of Pathology, Clinical Hospital Merkur, 4100 Zagreb, Croatia.

*Present address: Gene Expression Laboratory, Salk Institute for Biological Studies, 10010 North Torrey Pines Road, La Jolla, CA 92037, USA
†Author for correspondence (e-mail: Kemler@immunbio.mpg.de)

Accepted 27 October 2006

adhesive strength of E-cad was determined to be 3-4× higher than that of N-cad when cells expressing an equal amount of these two cadherins were compared (Chu et al., 2006; Chu et al., 2004).

Besides their similarities, E- and N-cad have in addition specific individual characteristics. N-cad function in particular appears to be cell context-dependent as it can induce cellular condensation, for example during chondrogenic differentiation, or induce morphological changes toward a more migratory phenotype. These unique functions of either N- or E-cad could largely depend on the context of interacting proteins. For example, E-cad can associate with the epidermal growth factor receptor (EGFR) (Fedor-Chaiken et al., 2003; Hazan and Norton, 1998; Hoschuetzky et al., 1994), whereas N-cad interacts with the fibroblast growth factor receptor (FGFR) (Byers et al., 1992; Williams et al., 1994) and promotes FGFR signal transduction. Both E- and N-cad are complexed via their cytoplasmic domains with catenins (α-, β-catenin, p120) (Aberle et al., 1996; Anastasiadis and Reynolds, 2000), key players in linking classical cadherins to the cytoskeleton. In addition, other interacting molecules, such as kinases and small GTPases, have been found to bind and modulate the function of the cadherin-catenin complex (Braga et al., 1999; Lickert et al., 2000; Lilien et al., 2002). Although not thoroughly examined, these cytoplasmic molecules could interact differently with E- or N-cad, resulting in different cellular responses. The modulation of the cadherin-catenin complex leads to changes in a number of important cellular processes, including reorganization of the cytoskeleton, formation of lamellipodia and cell migration (Ehrlich et al., 2002). These findings have advanced our knowledge of cadherin-mediated cell adhesion, but it should be noted that most of the results were obtained with cultured cells and so the biological significance in vivo remains to be clarified.

One of the central questions in cadherin and early mammalian developmental biology is: why does the organism strictly use only E- or N-cad, two highly related molecules, during specific, defined developmental processes? In order to address this question, we asked whether E- and N-cad are functionally identical and whether N-cad could function in an epithelial cell environment in vivo. We replaced E-cad with N-cad by inserting an *Ncad* cDNA into the *Ecad* locus using an established knock-in (k.i.) strategy (Stemmler et al., 2005). Here we show that when expressed from the *Ecad* locus, N-cad is localized to cells of the E-cad expression domains and displays a similar subcellular localization. However, although N-cad can rescue loss of E-cad for morula compaction, it is not able to substitute functionally for E-cad during the ensuing formation of trophectoderm. Thus, we demonstrate for the first time that although E-cad and N-cad have similar calcium-dependent adhesive properties, E-cad plays a unique role during early mouse development.

MATERIALS AND METHODS

Generation of N-cad knock-in mice by inserting *Ncad* (*Cdh2*) cDNA into the *Ecad* (*Cdh1*) genomic locus

To target the *Ecad* locus, k.i. targeting vectors containing cDNAs encoding N-cad or N-cad-GFP fusion protein were generated using standard cloning techniques (Sambrook and Russell, 1994). For the N-cad targeting vector, a genomic fragment of the mouse *Ecad* gene from –0.1 kb to +11 kb relative to the transcription start site was combined with an *Ecad* promoter fragment from –1.5 kb to –0.1 kb, together with an HSV-*tk* cassette (Stemmler et al., 2003). A cDNA encoding the mouse N-cad protein (Miyatani et al., 1989) was inserted into the ATG start codon of the *Ecad* gene, followed by a neomycin resistance gene, which was flanked by two *loxP* sites and driven in the opposite direction by the murine PGK promoter (Fig. 1A). Similarly, the N-cad-GFP targeting vector was generated using a modified cDNA coding for a C-terminally GFP-tagged N-cadherin protein (pEGFP-N3, Clontech). Homologous recombination at the *Ecad* locus was achieved by electroporation of 30 μg *Swa*I-linearized targeting vector DNA into E14.1 ES cells (Kuhn et al., 1991). Electroporated cells were subsequently subjected to positive/negative selection using G418 (Sigma, 300 μg/ml) and Gancyclovir (Cymeven, 2 μM). Positive clones were analyzed by PCR (see below) and Southern blot hybridization for correct and unique homologous recombination events using internal and external 5′ and 3′ probes (Fig. 1B). Two independent ES cell clones of each construct were used for injection into host C57BL/6 blastocysts. Chimeric males, identified by their coat color, were mated to C57BL/6 females to generate $Ecad^{+/Ncad}$ and $Ecad^{+/Ncad\text{-}GFP}$ mouse lines. After removal of the neomycin resistance cassette by mating with CMV-Cre deleter mice (Schwenk et al., 1995), $Ecad^{+/Ncad}$ and $Ecad^{+/Ncad\text{-}GFP}$ mice were backcrossed to C57BL/6.

Mouse breeding and genotyping

Heterozygous $Ecad^{+/Ncad}$ or $Ecad^{+/Ncad\text{-}GFP}$ embryos were obtained by crossings of k.i. lines to wild-type (wt) C57BL/6 mice. Preimplantation embryos were collected from heterozygous intercrosses of each line or from crossings of $Ecad^{fl/fl}$;$Zp3^{Cre/+}$ females to $Ecad^{+/Ncad\text{-}GFP}$ males to additionally remove maternal E-cad (Boussadia et al., 2002; De Vries et al., 2004).

Genotyping was performed by PCR with genomic DNA isolated from individual embryos or mouse tail biopsies using primers for the *Ncad* k.i. allele (E-cad5′UTR_s: CCAAGAACTTCTGCTAGAC and N-cad_as: TGGCAACTTGTCTAGGGA), *Ecad* wt allele (E-cad5′UTR_s/E-cad_as: TACGTCCGCGCTACTTCA), *Ecad* floxed allele [pE10.2/pE11as.2 (Boussadia et al., 2002)], *Cre-recombinase* (CAAGTTGAATAACCGG-AAATG and GCCAGGTATCTCTGACCAGA).

ES cell isolation and culture, embryo culture and blastocyst outgrowth analysis

ES cells were cultured on DR-4 feeder cells in ES cell medium [DMEM with 15% FCS, supplemented with 500 U/ml LIF (Chemicon, ESGRO #ES1107)]. Hetero- and homozygous N-cad-GFP k.i. ES cell lines were isolated from zona pellucida-free E2.5 embryos obtained from heterozygous intercrosses according to standard procedures (Doetschman et al., 1985). For in vitro culture, preimplantation embryos were flushed from oviducts or uteri at E2.5 or E3.5, respectively, in M2 medium (Sigma, M7167) and incubated in microdrops of KSOM medium (Specialty media, MR-020P-5F) under mineral oil (Fluka) for 24 or 48 hours and processed for time-lapse analysis or whole-mount immunofluorescence and subsequent genotyping. For blastocyst outgrowth analysis embryos were recovered at E2.5, treated with acidic Tyrode's solution (Sigma, T1788) to remove the zona pellucida and cultured in ES cell medium (see above) in gelatinized tissue culture chambers (Lab-tek, #177402) for 4 days. Blastocyst outgrowths were fixed and processed for whole-mount immunofluorescence.

Generation of chimeric embryos and β-galactosidase histochemistry

$Ecad^{+/Ncad\text{-}GFP}$ or $Ecad^{Ncad\text{-}GFP/Ncad\text{-}GFP}$ ES cells were injected into 129-*Gt(ROSA)26Sor/J* (ROSA26) (Soriano, 1999) or $Ecad^{+/Ncad}$; *Gt(ROSA)26Sor/J* E3.5 blastocysts and transferred to pseudopregnant females. Embryos were collected at E7.5 to E9.5, fixed in 1% formaldehyde/0.2% glutaraldehyde/PBS solution, then incubated overnight in X-gal staining solution, and processed as described previously (Stemmler et al., 2005).

Time-lapse microscopy

Time-lapse recordings were performed as described (Hiiragi and Solter, 2004). To record the morula compaction process, embryos were recovered at E2.5 and photographed every 30 minutes for 24 hours. To record blastocyst formation, embryos were recovered at E2.5, cultured in KSOM for 24 hours and then photographed every 30 minutes for another 24 hours. After recording, the DNA of individual embryos was recovered for genotyping.

RNA preparation and RT-PCR

RNA was isolated from individual or pooled embryos using the PicoPure RNA Isolation Kit (Arcturus, #KIT0204). cDNA was produced using Superscript II reverse transcriptase according to the manufacturer's instructions (Invitrogen). Specific transcripts were detected with primer combinations for *Ncad-GFP* (fw, GTGGGAATCAGACGGCTA and rev,

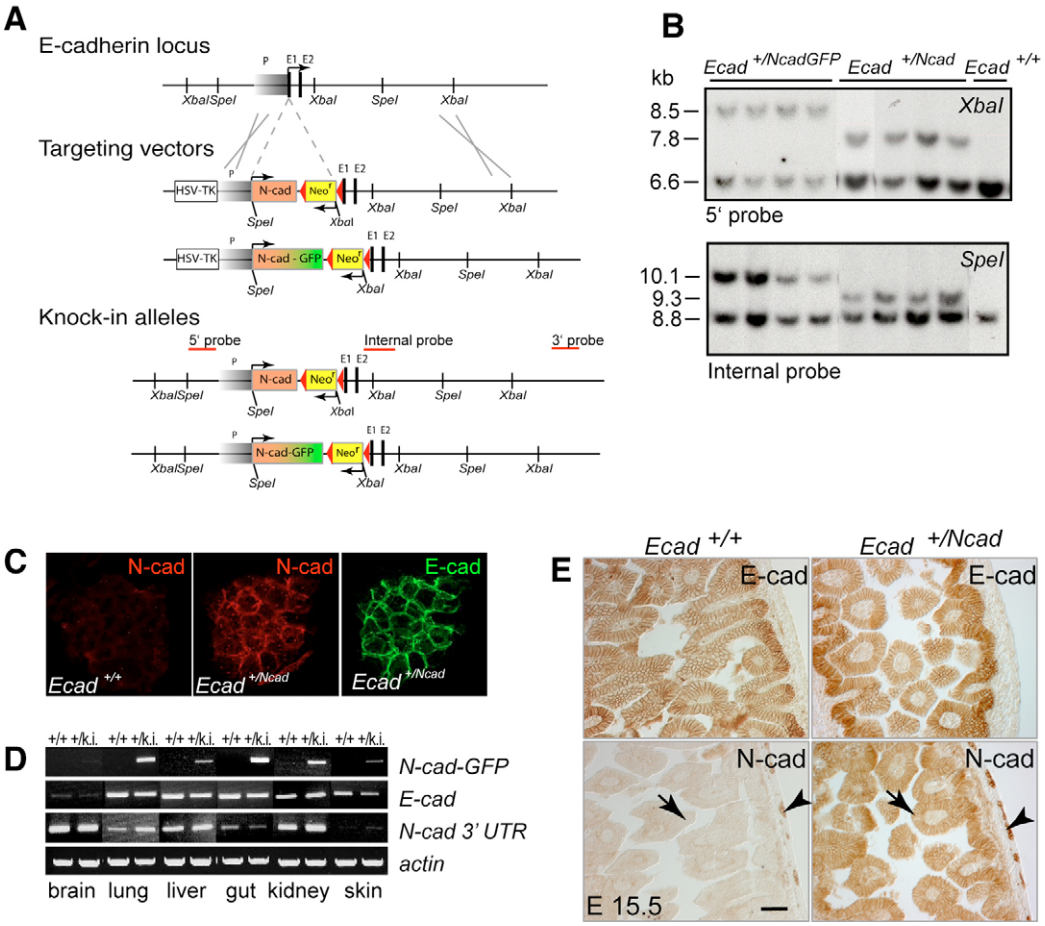

Fig. 1. Generation of *Ncad* k.i. mice. (**A**) Targeting strategy with schematic representation of the 5′ region of the *Ecad* genomic locus including promoter (P) and exons 1 and 2 (E1 and E2). Targeting vectors and expected recombined alleles are shown. Sites for restriction endonucleases and probes used are indicated. The neomycin selection cassette is flanked by two *loxP* sites (red triangles). (**B**) Southern blot analysis of targeted ES cell clones. DNA was digested with *Xba*I and probed with a 5′ probe (upper panel) located upstream of the targeting vectors (see also Fig. 1A). Fragments of 6.6 kb and either 7.8 kb or 8.5 kb were detected, corresponding to wt and *Ncad* k.i. or *Ncad-GFP* k.i. alleles, respectively. The internal probe was located downstream of exon 2. Fragments of 8.8 kb and either 9.3 kb or 10.1 kb, corresponding to wt and *Ncad* k.i. or *Ncad-GFP* k.i. alleles, respectively, were detected with *Spe*I-digested DNA (lower panel). Corresponding genotypes are indicated. (**C**) Double immunofluorescence against E- and N-cad on wt and targeted ES cell clones. N-cad is expressed from the k.i. allele and co-localizes with E-cad at the cell membrane. Wild-type ES cells are negative for N-cad immunoreactivity. (**D**) RT-PCR analysis of *Ncad-GFP* k.i. expression in different organs at E15.5. cDNAs from indicated organs of wt (+/+) or $Ecad^{+/Ncad}$ (+/k.i.) embryos were used with specific primers to amplify transcripts of *Ecad*, endogenous *Ncad* and *Ncad-GFP*. (**E**) Immunohistochemistry of wt and heterozygous *Ncad* k.i. embryos at E15.5. E-cad shows membrane localization in the intestine epithelium of wt and heterozygous *Ncad* k.i. embryos. N-cad k.i. protein is specifically detected in the intestinal epithelium of embryos carrying one *Ncad* k.i. allele but not in wt embryos (arrows). Endogenous N-cad protein is detected in peripheral muscle cells of the intestine in both wt and heterozygous embryos (arrowheads). Scale bar: 50 μm.

CCTCCTTGAAGTCGATGC), *Ecad* (fw, GAGCTGTCTACCAAAGTG and rev, TTCATCACGGAGGTTCCT), and *Ncad* 3′UTR (fw, AGTTTGGGCTCCCAGGGAATATCA and rev, CCTTTATCTGCAACCAGCTGCGTA).

Western blot analysis

Total protein was extracted from ES cells or tissue samples from E15.5 embryos with protein extraction buffer (25 mM HEPES, pH 7.4, 150 mM NaCl, 0.5% NP-40) and protease inhibitor cocktail (Roche), subjected to SDS-PAGE and transferred to a nitrocellulose membrane. Membranes were probed with mouse monoclonal anti-E-cadherin or anti-N-cadherin antibodies (see below) at a dilution of 1:3000 or 1:2500, respectively. Specific binding was detected with HRP-conjugated secondary antibodies (Jackson Laboratories) and visualized with ECL plus (Amersham, RNP2132).

Immunohistochemistry, whole-mount immunofluorescence and antibodies

Dehydrated, PFA-fixed embryos were embedded in paraffin wax and sectioned at 7 μm (Wilkinson and Green, 1990). Immunohistochemistry on paraffin sections was performed as described previously (Batlle et al., 2002). Whole-mount immunofluorescence on preimplantation embryos was performed as described (Kanzler et al., 2003) with the following modifications. All procedures were carried out at room temperature. Embryos were fixed for 20 minutes in 2% PFA in PBS containing 0.05% Tween 20 (PBT). After permeabilization for 20 minutes with 0.25% Triton X-100 in PBS and several washes in PBT, embryos were blocked for 20 minutes with 2% goat serum in PBT and then incubated for 1 hour with primary antibodies. After intensive washes, embryos were incubated for 30 minutes with secondary antibodies, washed, mounted in microdrops on a glass-bottom dish and analyzed by confocal microscopy (see below).

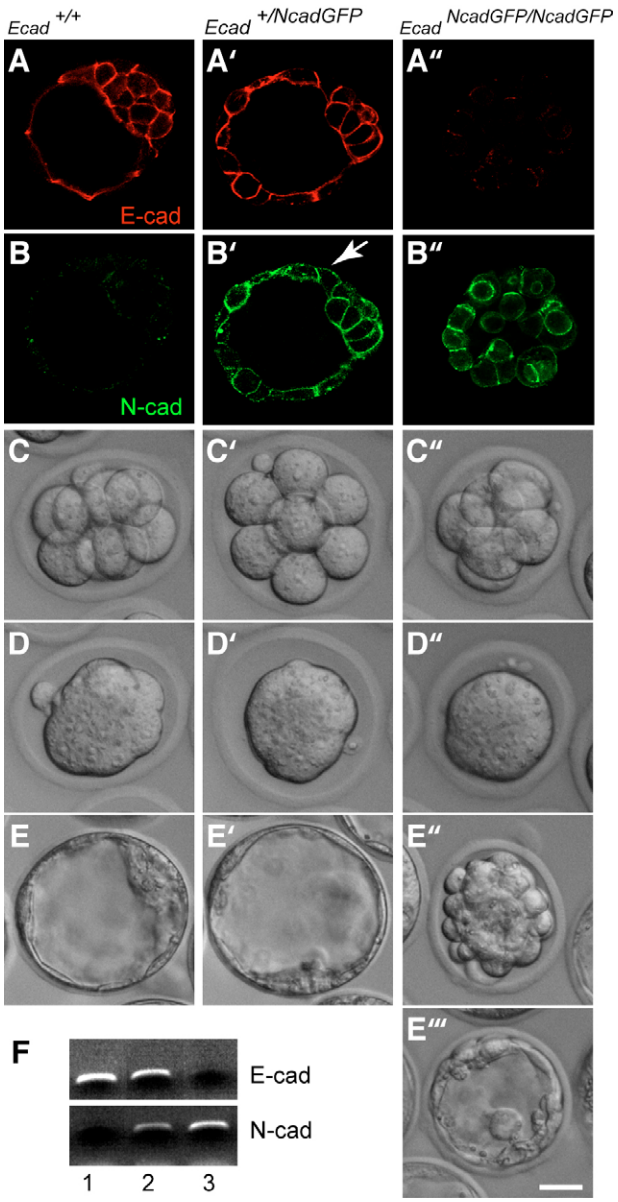

Fig. 2. Homozygous *Ncad* k.i. mutants fail to form an intact trophectoderm. (**A-B″**) Double immunolabeling of E- and N-cad protein. E-cad is localized at the cell-cell contact sites in wt (A) and heterozygous *Ncad* k.i. E4.5 blastocysts (A′), but is absent in homozygous *Ncad* k.i. embryos (A″). N-cad immunolabeling is observed in heterozygous (B′) and homozygous mutants (B″). No N-cad staining above background is observed in wt embryos (B). Co-localization of E- and N-cad at cell-cell contact sites of both ICM and TE is seen in heterozygous preimplantation embryos (A′,B′). Additional punctate staining of N-cad is seen on the apical membrane of TE cells (B′, arrow). (**C-E‴**) Time-lapse analysis of the preimplantation development of *Ncad* k.i. embryos. Recordings were started at the 8-cell stage (C-C″) and continued for 24 hours. Representative pictures of recordings are shown. At the 8-cell stage, wt (C), heterozygous (C′) and homozygous (C″) embryos were indistinguishable, and all developed normally to compacted morulae (D-D″). (E-E‴) Representative pictures of in vitro-cultured E4.5 embryos. Wt (E) and $Ecad^{+/Ncad}$ (E′) embryos formed expanded blastocysts, whereas homozygous $Ecad^{Ncad/Ncad}$ mutants showed loosening of cell-cell contacts and formed either no cavity (E″) or only small cavity-like cysts (E‴). (**F**) RT-PCR analysis of single E3.5 blastocysts: wt (1), heterozygous (2) and homozygous k.i. (3) embryos with primers for *Ecad* and *Ncad* mRNA as indicated. Scale bar: 25 μm.

The following antibodies were used. Mouse anti-N-cadherin (1:200, BD Transduction Laboratories, #610921), mouse monoclonal anti-E-cadherin (1:200, BD Transduction Laboratories, #610182), mouse monoclonal anti-β-catenin (1:200, BD Transduction Laboratories, #610154), polyclonal rabbit anti-ZO1 (1:200, Zymed, #617300), affinity-purified rabbit anti-gp84 antibody against the extracellular domain of E-cadherin (1:200) (Vestweber and Kemler, 1984), rat monoclonal antibody TROMA-1 against cytokeratin 8 (1:20) (Kemler et al., 1981), rabbit anti-ezrin (1:200) which was a kind gift of Paul Mangeat (Andreoli et al., 1994), polyclonal rabbit anti-PKCζ (1:300, Santa Cruz, sc-216), mouse monoclonal anti-Oct4 (1:200, Santa Cruz, sc-5279), polyclonal rabbit anti-Cdx2 (1:100) which was a kind gift of Felix Beck (Beck et al., 2003), mouse monoclonal anti-myogenin (1:50, Abcam, ab1835), mouse monoclonal anti-β-tubulin III (1:200, Sigma, T8660), mouse monoclonal anti-GFAP (1:200, Sigma, G3893), mouse monoclonal anti-neurofilament 160 (1:50, Sigma, N5264), mouse monoclonal anti-nestin (1:5, DSHB, Rat-401), mouse monoclonal anti-GFP (1:100, Roche, #11814460001), Alexa-488-labeled rabbit anti-GFP (1:100, Molecular Probes, A21311). For mouse and rabbit antibodies the DAKO Envision+ System HRP was used as a secondary reagent (DakoCytomation, K4000 and K4002). For rat antibodies, secondary peroxidase-conjugated anti-rat IgG antibody (1:100, Jackson ImmunoResearch Laboratories, 312-035-003) was used. Staining of paraffin sections was visualized with DAB Peroxidase Substrate (Sigma, D-4293). For immunofluorescence, secondary species-specific Alexa-fluorochrome-conjugated antibodies were used at a dilution of 1:300 (Molecular Probes). To detect actin filaments, embryos were stained with Alexa-Fluor 488 Phalloidin (1:200, Molecular Probes, A12379). Nuclei were visualized with DAPI (1:1000, Molecular Probes, D3571).

TUNEL staining

Isolated compacted morulae or E3.5 blastocysts were fixed in 2% paraformaldehyde in PBS for 20 minutes at room temperature, washed with PBT (PBS plus 0.05% Tween 20), and incubated in TUNEL reaction mixture according to the manufacturer's instructions (Roche, In Situ Cell Death Detection Kit, #1684795). Nuclei were co-stained with DAPI.

Teratoma production

1×10^7 ES cells were injected subcutaneously into 6-8 week-old nude mice in a single-cell suspension. Teratomas were isolated between 3.5 and 5.5 weeks after injection, and split into two parts for DNA purification and paraffin embedding.

Confocal microscopy

Confocal analysis was performed using a Leica TCS SP2 UV laser scan head attached to a Leica DM IRE2 inverted microscope equipped with Leica Confocal software version 2.5. Optical sections were taken every 2 μm. 3D images were reconstructed in IMARIS imaging software version 4.05 (Bitplane AG).

RESULTS

Generation of knock-in mice by insertion of *Ncad* cDNA into the *Ecad* genomic locus

In order to investigate the functional similarities and differences between the two classical cadherins, we genetically replaced *Ecad* by *Ncad*. Two targeting vectors were used to insert either *Ncad* cDNA or a fusion construct composed of *Ncad* and green fluorescent protein (*Ncad-GFP*) at the start codon of the *Ecad* locus. This targeting strategy was successfully used previously to insert a *betageo* reporter gene that resulted in the expression of β-galactosidase specifically in the E-cad expression domains, thus indicating that all endogenous regulatory sequences were still intact after targeting and hence could control correct tissue-specific expression (Stemmler et al., 2005).

A scheme for the targeting of the *Ecad* genomic locus, as well as the diagnostic probes for Southern blot analysis, are depicted in Fig. 1A. Homologous recombination was observed in about 10% of ES cell clones analyzed by Southern blot analysis (Fig. 1B). Homologously recombined ES cell clones expressed N-cad-GFP protein, which was co-localized with E-cad at the cell membrane (Fig. 1C). Two independent clones from each targeting vector were used for blastocyst injection to generate chimeric males. Founders were bred with CMV-Cre deleter females to remove the floxed neomycin gene (Neo^r in Fig. 1A). Heterozygous offspring of both lines ($Ecad^{+/Ncad}$ or $Ecad^{+/Ncad\text{-}GFP}$) were phenotypically normal and transmitted the k.i. allele in a mendelian ratio. Transcription and protein expression of both k.i. alleles were studied during the development of heterozygous embryos. Comparable results were obtained for N-cad-GFP (Fig. 1D) and N-cad k.i. alleles (Fig. 1E). Using specific primers to *Ncad-GFP* coding sequence or to the *Ncad* 3′UTR sequences, *Ncad-GFP* was found by RT-PCR to be co-expressed together with *Ecad* mRNA in lung, liver, gut, kidney and skin. In brain, where E-cad is not expressed at high level, N-cad-GFP expression was also very weak as compared with the high level of endogenous N-cad expression (Fig. 1D).

We then analyzed tissue-specific expression and membrane localization by immunohistochemistry on sections of E15.5 embryos (Fig. 1E). E-cad exhibited the known membrane localization in the villi and crypt region of the small intestine in both wt ($Ecad^{+/+}$) and the N-cad k.i. littermates ($Ecad^{+/Ncad}$). N-cad was also detected in intestinal epithelial cells in heterozygous embryos ($Ecad^{+/Ncad}$), but not in the intestine of wild-type embryos (Fig. 1E, arrows). By contrast, endogenous N-cad was found in the peripheral muscles and the enteric nervous system of the intestine (Fig. 1E, arrowheads). Co-expression and membrane localization of N-cad derived from the k.i. allele, together with endogenous E-cad, were also observed in epithelial cells of lung, kidney, lens epithelium, adrenal and pancreatic glands, liver and skin (not shown). These results clearly demonstrate that with the k.i. strategy employed, expression of N-cad is directed to the E-cad expression domains. Moreover, E- and N-cad can be co-expressed in epithelial cells in vivo without any obvious perturbation of epithelial cell integrity.

Embryos homozygous for N-cad cannot form an intact trophectoderm

In order to ascertain to what extent N-cad can substitute for E-cad, heterozygous animals were intercrossed with a view to analyzing the developmental potential of embryos homozygous for the *Ncad* k.i. allele. However, no homozygous k.i. mutant embryos were recovered post-implantation (E5.5-E7.5). Each litter included deciduae which were empty or filled with cellular debris, suggesting that homozygous mutant embryos induced a decidual reaction, but failed to undergo further development.

These results pointed to lethal developmental defects during preimplantation development. To test if transcripts from the k.i. allele were already expressed in preimplantation embryos, single E3.5 blastocysts from heterozygous intercrosses were subjected to RT-PCR analysis. Transcripts from the *Ncad* k.i. allele were detected in both heterozygous and homozygous embryos (Fig. 2F, lanes 2 and 3, respectively), whereas endogenous N-cad was not expressed in wt embryos at this developmental stage (Fig. 2F, lane 1). In early-stage heterozygous blastocysts, N-cad-GFP and E-cad were co-localized at the membrane of cells in the trophectoderm and the inner cell mass (ICM) (Fig. 2A′ and B′, respectively). Interestingly, in the trophectoderm, N-cad-GFP exhibited baso-lateral membrane localization similar to E-cad. Some punctate staining for N-cad-GFP was also observed on the apical membrane of the trophectoderm (Fig. 2B′, arrow). Apparent immunohistochemical differences in the relative staining intensity of E- versus N-cad might merely reflect differences between the antibodies used for detection: E-cad was stained with rabbit affinity-purified antibodies directed against the extracellular

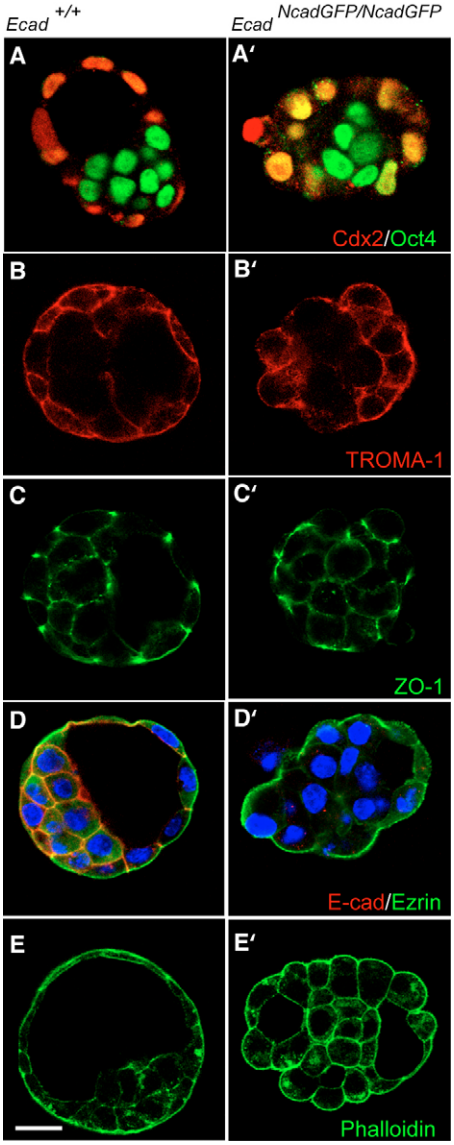

Fig. 3. Expression of trophectodermal and lineage specification markers in *Ncad* k.i. mutants. (**A**,**A′**) Double immunolabeling of E3.5 embryos with antibodies against Oct4 (green) and Cdx2 (red) shows predominantly ICM localization of Oct4 and trophectodermal expression of Cdx2 in wt (A) and in mutant embryos (A′). Some outer cells are also Oct4-positive in mutant embryos (A′). (**B**,**B′**) Monoclonal TROMA-1 antibody detects intermediate filament marker cytokeratin 8 in mutant (B′) and wt (B) embryos. (**C**,**C′**) Immunolocalization of ZO-1. In wt embryos ZO-1 localization is restricted to tight junctions (C). More extended and less punctate membrane localization of ZO-1 protein is seen in homozygous $Ecad^{Ncad\text{-}GFP/Ncad\text{-}GFP}$ mutants (C′). (**D**,**D′**) Polyclonal anti-ezrin antibodies were used to detect microvilli on the apical pole of the outer cells in compacted wt (D) and mutant (D′) embryos. (**E**,**E′**) Actin cytoskeleton was detected with Alexa-488-conjugated Phalloidin. Scale bar: 25 μm.

domain of the protein (anti-gp84), whereas N-cad and N-cad-GFP were detected with monoclonal antibodies raised against the cytoplasmic domain of N-cad.

The preimplantation development of homozygous mutant, heterozygous and wt embryos was recorded by time-lapse microscopy prior to genotyping. To minimize any possible damage caused by the recording procedure, time-lapse analysis was performed in two steps: from 4- to 8-cell embryos to compacted morulae and from morulae (E3.5) to blastocysts (E4.5). DIC images were taken every 30 minutes (see Movies 1-4 in the supplementary material). Representative images from the recordings are provided in Fig. 2C-E‴. All embryos developed into compacted morulae independent of the genotype (Fig. 2D,D′,D″) and no obvious delay in cleavage and/or the onset of compaction was observed in embryos homozygous for the *Ncad* k.i. allele. In addition, no differences were found with respect to cell numbers or apoptosis among the three genotypes (not shown). However, clear morphological differences became visible between E3.5 and E4.5, when wt and heterozygous embryos had formed blastocysts (Fig. 2E,E′). At this time-point, homozygous mutant embryos were unable to form an intact trophectoderm, although they had undergone compaction (Fig. 2E″,E‴). In most of the mutant embryos, the outer cells rounded up with clear signs of reduced cell-cell contacts (Fig. 2E″). When E3.5 to E4.5 homozygous mutant embryos were stained for N-cad-GFP, the protein predominantly localized to cell-cell contact sites, becoming more irregularly distributed between the membrane and in the cytoplasm as the mutant phenotype became more apparent (Fig. 2B″). Only occasionally did an outer cell layer separate from the inner cells and small cavity-like cysts form (Fig. 2E‴). Even with prolonged culture, homozygous mutant embryos never hatched from the zona pellucida and many cells vacuolized and died. Thus, the phenotype of the *Ncad-GFP* k.i. mutant is remarkably similar to that of classical E-cad-null mutant embryos (Larue et al., 1994).

Differentiation marker analysis and trophectoderm outgrowth of N-cad-GFP mutant embryos

Normally, during the transition from morula to blastocyst, the outer cell layer of the embryo polarizes and starts to express a variety of epithelial cell-specific genes required for the future trophectoderm.

To determine if the expression of epithelial cell-specific genes is altered in *Ncad-GFP* mutant embryos, immunohistological analysis was performed, with subsequent genotyping of each embryo. The transcription factors Cdx2 and Oct4 (Pou5f1 – Mouse Genome Informatics) specify the trophectodermal and ICM lineages, respectively, in wt blastocysts (Fig. 3A), although some trophectodermal cells still co-express Cdx2 and Oct4 in E3.5 blastocysts (not shown). In $Ecad^{Ncad/Ncad}$ mutant embryos, Oct4 was also preferentially localized in nuclei of inner cells, whereas Cdx2 was found in outer cells, although co-localization could be seen to some extent (Fig. 3A′). These results suggest that an epithelial cell-specific program is initiated in the outer cells of mutant embryos. This interpretation was further supported by the finding that the outer cells expressed several epithelial markers (Fig. 3B-E′). As in wt embryos, the intermediate filament protein cytokeratin 8 (keratin 8 – Mouse Genome Informatics) was expressed by the outer cells of homozygous embryos (Fig. 3B,B′). Furthermore, the tight junction protein ZO-1 (Tjp1 – Mouse Genome Informatics) showed a typical punctate localization in the trophectoderm of wt embryos (Fig. 3C). In homozygous mutant embryos, ZO-1 was less punctate and more extended along the lateral membrane of outer cells (Fig. 3C′). Other epithelial cell-specific markers, such as occludin, PKC-zeta (Prkcz – Mouse Genome Informatics) and desmosomal cadherins, were also expressed in the outer cells of homozygous mutant embryos (not shown). Ezrin (villin 2 – Mouse Genome Informatics), a member of the ERM protein family, links the actin cytoskeleton to the plasma membrane and is involved in the formation and stabilization of the apical microvillus pole during morula compaction (Louvet et al., 1996). In early mutant embryos, ezrin was localized at the apical pole of outer cells, similar to the distribution found in normal embryos (Fig. 3D,D′). At later stages, between E4.0-E4.5, when the mutant phenotype became apparent, ezrin also localized to the baso-lateral membrane (not shown). Actin cytoskeleton staining with Phalloidin gave similar results. Actin was found to be concentrated at the apical pole of outer cells in wt and mutant embryos, but also at the baso-lateral membrane of advanced-stage mutant embryos (Fig. 3E′; for wt, see E). Mutant embryos died within the zona pellucida, which hampered further analysis of their differentiation potential.

To address the question whether, under in vitro conditions, outer cells of the homozygous N-cad k.i. mutant could further differentiate into trophoblast cells, the zonae pellucidae of mutant and wt E2.5 embryos were removed and the embryos cultured on gelatin-coated dishes. In both cases, trophoblast outgrowths containing giant cells were observed (Fig. 4A,A′, arrows). Although E-cad was detected in only $Ecad^{+/+}$ ICMs (Fig. 4B,B′), outgrowths were positive for cytokeratin 8 in both cases (Fig. 4C-D′). Remarkably, mutant embryos formed an ICM on top of the attached trophectoderm (Fig. 4A′, arrowhead), and this allowed us to establish ES cell lines.

These results show that, in embryos expressing N-cad-GFP from the *Ecad* locus, inside and outside blastomeres can be distinguished by molecular markers, and outside cells exhibit many features of normal trophectodermal cells. Although outer cells start to polarize, polarization is not maintained in mutant embryos. A possible drawback of these experiments is that some maternal E-cad is present in the mutant embryos that could contribute to compaction and possibly to the onset of differentiation.

Mutant N-cad-GFP embryos lacking maternal E-cad

Zygotic *Ecad* gene inactivation has revealed that maternal E-cad can mediate compaction at morula stage (Larue et al., 1994; Ohsugi et al., 1997). Depletion of the maternal E-cad resulted in the dissociation of blastomeres, but adhesion and compaction could be rescued by the paternal *Ecad* allele (De Vries et al., 2004). Thus, it was important to study the possible contribution of maternal E-cad to the *Ncad-GFP* mutant phenotype, particularly in the polarization and the expression of epithelial markers in the outer cells of mutant embryos. Using a zona pellucida glycoprotein 3 promoter-driven Cre recombinase in combination with a floxed *Ecad* allele, we were able to inactivate the maternal *Ecad* gene specifically during oocyte maturation (De Vries et al., 2004). Such females were crossed with $Ecad^{+/Ncad\text{-}GFP}$ males to produce $Ecad^{-/+}$ or $Ecad^{-/Ncad\text{-}GFP}$ embryos. Time-lapse recording was performed between E2.5 and E4.0, and representative pictures are shown in Fig. 5A-B′. Interestingly, both $Ecad^{-/+}$ and $Ecad^{-/Ncad\text{-}GFP}$ embryos compacted around E3.0 (Fig. 5A,A′). Since both the *Ecad* wt and the *Ncad-GFP* alleles are paternal, this result indicates that the *Ncad-GFP* allele can also rescue the initial cell adhesion defect caused by the lack of maternal E-cad. However, thereafter, the N-cad-GFP protein was unable to maintain the formation of an intact trophectoderm, as was also the case for E-cad encoded by the paternal allele (Fig. 5B,B′).

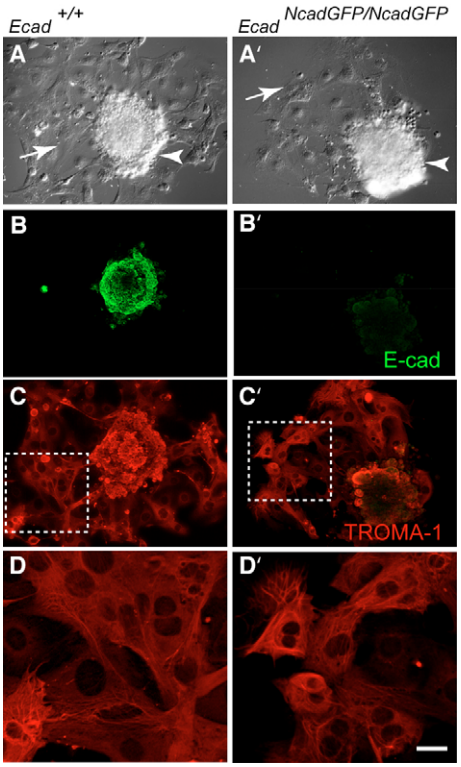

Fig. 4. *Ncad* k.i. embryos can attach and form blastocyst outgrowth. DIC images of wt (**A**) and *Ecad*$^{Ncad\text{-}GFP/Ncad\text{-}GFP}$ (**A′**) blastocyst outgrowths. Homozygous mutant embryos were able to attach and differentiate into trophoblast giant cells (arrow) and ICM (arrowhead). E-cad is expressed in the ICM and downregulated in giant cells of wt embryos (**B**) and is absent in the ICM of homozygous mutant embryos (**B′**). The trophoblast marker antibody TROMA-1 stained cells of both wt and mutant outgrowths (**C-D′**). D,D′ are enlarged pictures of the outlined areas in C,C′, respectively. Scale bar: 100 μm.

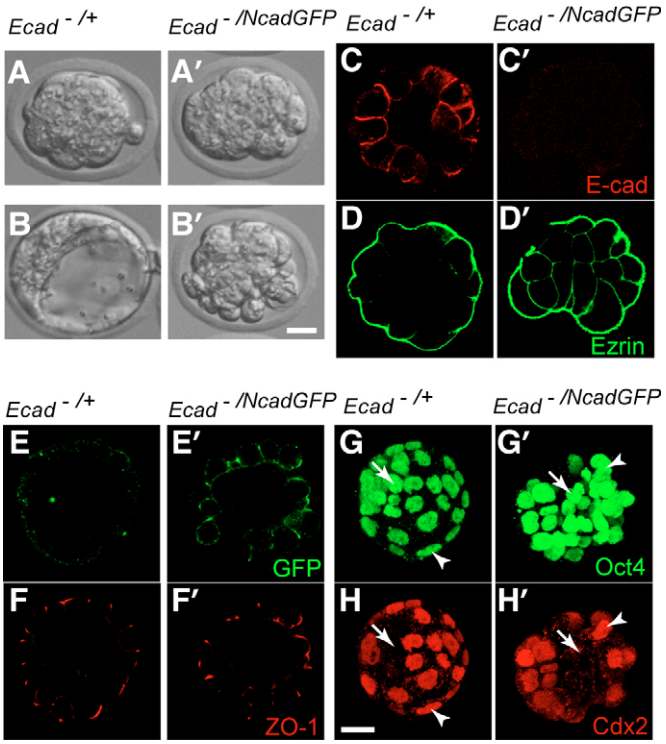

Fig. 5. Development of *Ncad-GFP* k.i. embryos in the absence of maternal E-cad. Representative pictures of time-lapse recordings showing embryos without maternal E-cad but expressing paternal E-cad (*Ecad*$^{-/+}$) (**A**,**B**) or expressing N-cad-GFP from the k.i. allele (*Ecad*$^{-/Ncad\text{-}GFP}$) (**A′**,**B′**). Both embryos compact in a similar fashion around E3.0 (A,A′). By E4.0, embryos expressing paternal E-cad develop to early blastocyst (B), whereas embryos expressing paternal N-cad-GFP from the k.i. allele begin to deteriorate shortly after compaction (B′). Immunolabeling shows expression and membrane localization of E-cad from the paternal allele in *Ecad*$^{-/+}$ embryos (**C**) and no E-cad expression in embryos carrying a paternal *Ncad-GFP* k.i. allele (**C′**). The same embryos were co-stained with a polyclonal anti-ezrin antibody (**D**,**D′**). Expression of N-cad-GFP was confirmed by immunostaining with a monoclonal anti-GFP antibody (**E′**). Only low levels of background staining are seen in embryos with a paternal E-cad allele (**E**). Embryos shown in E and E′ were co-stained for ZO-1 (**F**,**F′**). (**G-H′**) Oct4 and Cdx2 are expressed in *Ncad-GFP* k.i. embryos in the absence of maternal E-cad. 3D-reconstruction pictures from multiple optical sections show nuclear localization of Oct4 mostly in the ICM of *Ecad*$^{-/+}$ early blastocyst (G) and inner cells of *Ecad*$^{-/Ncad\text{-}GFP}$ morulae (G′). Cdx2 is expressed exclusively in outer cells in both *Ecad*$^{-/+}$ (H) and *Ecad*$^{-/Ncad\text{-}GFP}$ (H′) embryos. Co-expression of Oct4 and Cdx2 is still observed in trophectodermal cells of E3.5 embryos. Arrows show ICM, arrowheads show TE. Scale bar: 25 μm.

Immunofluorescence clearly demonstrated that the paternally-encoded E-cad and N-cad-GFP proteins localize to the baso-lateral membrane of outer cells (Fig. 5C,E′). Cell-cell contacts in the outer cells appeared to be more dense in the presence of E-cad than of N-cad-GFP alone. In agreement with previous experiments, double-labeling revealed that in embryos expressing N-cad-GFP, the tight junction protein ZO-1 localized correctly to the outer cells (Fig. 5F′). However, staining for ezrin revealed a clear difference between *Ncad-GFP* mutant embryos with or without maternal E-cad (compare Fig. 3D′ with Fig. 5D′). In embryos lacking maternal E-cad and expressing only the paternal *Ncad-GFP* allele, ezrin was concentrated less distinctly at the apical pole of the outer cells and was localized at the baso-lateral membrane (Fig. 5D′). In control embryos expressing only the paternal *Ecad* allele, ezrin localized specifically to the apical pole of outer cells (Fig. 5D). These results indicate that the paternal N-cad-GFP cannot efficiently induce and maintain polarization of the outside cells even though they express some epithelial markers. Staining for Oct4 and Cdx2 revealed partial co-expression (Fig. 5G-H′), although Cdx2 protein was largely found in the nuclei of outer cells (Fig. 5H,H′). Taken together, embryos without maternal E-cad and expressing only paternal N-cad-GFP can compact but show an impaired maintenance of polarization, even though outside cells express epithelial cell markers.

Differentiation potential of ES cells homozygous for *Ncad-GFP*

Embryos homozygous for the *Ncad* k.i. allele die at blastocyst stage because of incomplete trophectoderm formation. Several attempts were undertaken to overcome this developmental block and thereby to study the subsequent differentiation potential of cells expressing N-cad-GFP instead of E-cad. First, morula aggregation using wt, *Ecad*$^{+/Ncad\text{-}GFP}$ and *Ecad*$^{Ncad\text{-}GFP/Ncad\text{-}GFP}$ embryos was attempted. Although cells from *Ecad*$^{+/Ncad\text{-}GFP}$ and wt embryos intermixed well and formed blastocysts, no cell mixing was observed between wt embryos and embryos homozygous for *Ncad-GFP* (not shown).

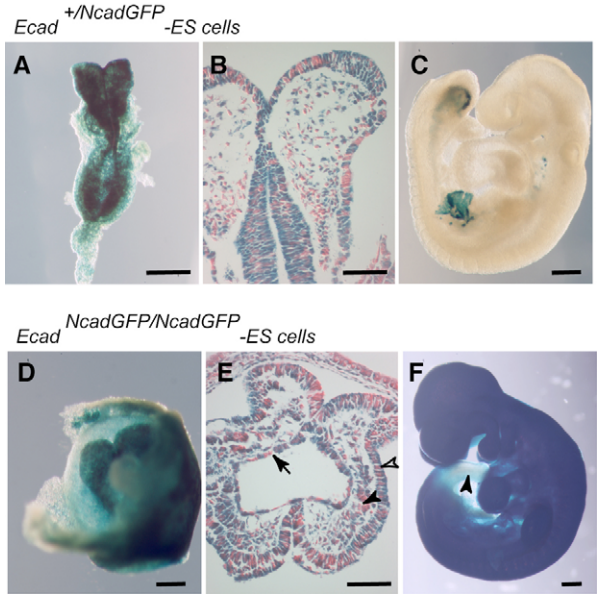

Fig. 6. *Ecad*$^{Ncad\text{-}GFP/Ncad\text{-}GFP}$ ES cells can contribute to forming chimeric embryos. (**A-C**) Representative X-gal stained embryos obtained from injection of *Ecad*$^{+/Ncad\text{-}GFP}$ ES cells into ROSA26 (*ROSA26;Ecad*$^{+/+}$) blastocysts that constitutively express *lacZ*. Chimeric embryos with contribution of ES cells (17 of 33 analyzed embryos showed chimerism with average ES cell contribution of 50-90%) were identified by unstained cells. (A) E8.5 chimeric embryo with approximately 50% ES cell contribution. *Ecad*$^{+/Ncad\text{-}GFP}$ ES cells can contribute to all germ layers as seen in sections at E8.5 (B). (C) E9.5 chimeric embryo with 90% ES cell-derived cells. (**D-F**) X-gal staining of embryos derived from injections of *Ecad*$^{Ncad\text{-}GFP/Ncad\text{-}GFP}$ ES cells into ROSA26 blastocysts. In 15 of 52 analyzed embryos, ES cell-derived cells are detectable, with an average contribution to the host embryo of 5-20%. Representative embryos at E8.5 with even distribution (D) and with contribution mainly to the tail at E9.5 (F, arrowhead) are shown. (E) Sections of the embryo in D revealed greater than 20% ES cell contribution to all germ layers (arrow, endoderm; black arrowhead, mesoderm; white arrowhead, ectoderm). Scale bars: A,C,F, 500 μm; B,D,E, 100 μm.

Both partner embryos remained separated, with the wt embryo forming a blastocyst next to the arrested mutant embryo. Taking another approach, ES cells homozygous for *Ncad-GFP* were established from preimplantation embryos (see Fig. 4A′). Homozygous *Ncad-GFP* ES cells exhibited typical ES cell morphology, indicating that N-cad-GFP can maintain cell-cell contacts between these cells (see Fig. S1 in the supplementary material). Mutant ES cells homozygous for *Ncad-GFP* were used for aggregation experiments with a tetraploid embryo as partner. As in the case of the morula aggregation, cells expressing N-cad-GFP did not intermix with wt cells expressing E-cad (data not shown). Thus, neither approach allowed us to characterize the complete differentiation potential of the *Ncad-GFP* mutant ES cells. In an alternative approach, ES cells homozygous or heterozygous for *Ncad-GFP* were injected into ROSA26 blastocysts to produce chimeric embryos (Fig. 6). To circumvent possible intermixing problems mentioned above, we also used *ROSA26;Ecad*$^{+/Ncad}$ blastocysts as host. ES cells heterozygous for *Ncad-GFP* contributed to all three germ layers (Fig. 6B) and chimeric embryos with 50-90% ES cell contribution were observed (Fig. 6A,C). By contrast, the contribution of homozygous N-cad-GFP ES cells was significantly lower. It was noted that chimeric embryos with a strong contribution of homozygous mutant ES cells exhibited major malformations already detectable at E7.5 (not shown). However, chimeric embryos with lower homozygous mutant ES cell contribution (5-20%, Fig. 6D,F) and normal morphology (15 out of 52 analyzed) showed ES cell integration into all three germ layers (Fig. 6E). Similar results were obtained when *ROSA26;Ecad*$^{+/Ncad}$ host blastocysts were used (54 embryos analyzed, not shown). These results demonstrate that homozygous *Ncad-GFP* ES cells can participate in all three germ layers, particularly in the formation of surface ectoderm in chimeric embryos.

To further characterize the differentiation potential of homozygous *Ncad-GFP* ES cells, teratomas were generated. When injected subcutaneously into syngenic or nude mice, ES cells form benign teratomas, which are composed of a large variety of differentiated cell types and tissue-like structures. Teratomas were obtained from *Ecad*$^{+/Ncad\text{-}GFP}$ and *Ecad*$^{Ncad\text{-}GFP/Ncad\text{-}GFP}$ ES cells (Fig. 7A,A′, respectively), sectioned and subjected to histological and immunohistochemical analysis (Fig. 7 and see Fig. S2 in the supplementary material). Histological examination revealed that *Ncad-GFP* homozygous ES cells generated a large variety of tissue-like structures, notably muscle bundles, brain tissue, including primitive neural tubes, and gland-like structures (Fig. 7A′ and see Fig. S2 in the supplementary material). Importantly, several different epithelial-like structures were observed, such as respiratory epithelia, squamous epithelia with signs of keratinization, and secretory epithelia with goblet cells (Fig. 7A′ and see Fig. S2A-D in the supplementary material). Most remarkably, in *Ncad-GFP* homozygous teratomas, the epithelial structures expressed N-cad-GFP and not E-cad, as visualized in consecutive sections (Fig. 7B′,C′). These epithelial structures also expressed cytokeratin 8 (TROMA-1 in Fig. 7D′). In sections obtained from control heterozygous *Ecad*$^{+/Ncad\text{-}GFP}$ teratomas, these epithelial structures co-expressed E-cad and N-cad-GFP (Fig. 7B,C) and were positive for TROMA-1 antibody staining (Fig. 7D). Staining for differentiation markers revealed that teratomas obtained from homozygous *Ncad-GFP* ES cells expressed neuronal markers, such as GFAP and neurofilaments, but also the muscle differentiation marker myogenin (see Fig. S2E-G′ in the supplementary material). These data clearly show that homozygous N-cad-GFP ES cells can differentiate into a large variety of different cell types and can form tissue-like structures similar to those generated in teratomas from wt or *Ncad-GFP* heterozygous ES cells. Most notably, homozygous mutant ES cells differentiate into epithelial structures that express N-cad-GFP.

DISCUSSION

During mouse preimplantation development, the fertilized egg undergoes several cell divisions, and at the 32-cell stage forms a blastocyst consisting of a fluid-filled cyst of trophectodermal epithelium (TE) that invades the uterine epithelium and contributes to the placenta, and an ICM that will generate the embryo proper. This process can be traced back to a morphological reorganization called compaction that starts at the 8-cell stage with increased intercellular adhesion, and proceeds as a dynamic process that is established gradually over three cell cycles. At compaction, outer polarized blastomeres segregate from the inner, non-polarized cells and progressively differentiate and assemble typical epithelial intercellular junctions. The cell adhesion molecule E-cad plays a crucial role in these early differentiation processes. Lack of zygotic E-cad leads to a non-functional trophectoderm, but mutant embryos can still compact owing to maternally-derived *Ecad* mRNA and

protein (Larue et al., 1994; Ohsugi et al., 1997). Elimination of maternal E-cad by conditional germline gene inactivation results in a complete loss of cell adhesion from the 2-cell stage onward (De Vries et al., 2004).

In the present study, we asked to what extent N-cad is able to replace E-cad function when it is expressed in vivo in the E-cad expression domain. We employed a gene k.i. strategy and generated heterozygous mice where N-cad is co-expressed with E-cad. Heterozygous mice were indistinguishable from wt littermates and did not show any obvious developmental or physiological abnormalities. Detailed analysis revealed that the expression of N-cad protein derived from the k.i. allele recapitulated the E-cad spatio-temporal expression pattern, which confirms our earlier observations of a faithful pattern of expression with a k.i. of a *lac*Z reporter gene using the same targeting strategy. Our results clearly demonstrate that N-cad synthesized from the *Ecad* locus is expressed on the cell surface and confers cell-cell adhesion. In epithelia of heterozygous ($Ecad^{+/Ncad}$) embryos, both E- and N-cad exhibit a superimposable baso-lateral membrane distribution. Since E- and N-cad exhibit unique and mostly mutually exclusive spatio-temporal expression patterns in wt mice, it is important to note that the co-expression of N-cad and E-cad in E-cad expression domains did not affect embryonic development. Although we cannot rule out that N-cad derived from the k.i. allele is present at lower levels than the endogenous E-cad would be, potentially as a result of differences in protein and RNA stability, we believe that use of the endogenous *Ecad* locus to express N-cad was the most appropriate approach to address the question of functional interchangeability. Continuing analysis should tell us to what extent N-cad contributes to adherens junctions and if lateral heterodimers with E-cad can be formed. The heterozygous mice will be of interest, generating epithelia that express only N-cad by conditionally deleting E-cad in these cells.

The most surprising result of our study is that embryos homozygous for the *Ncad* k.i. allele phenocopy the classical *Ecad* knockout. This suggests that E-cad has specific properties for trophectoderm formation which N-cad cannot provide. This view is supported by experiments in which *Ecad* cDNA was introduced by the same k.i. strategy. Homozygous *Ecad* k.i. embryos can form blastocysts and implant (M.S., unpublished). As with E-cad-null mutants, embryos homozygous for the *Ncad* k.i. allele undergo compaction, and the outer cells initiate epithelial polarization. This is accompanied by the normal expression of genes such as ezrin and *aPkc* (*Prkca* – Mouse Genome Informatics) and epithelial cell-specific genes, such as cytokeratin 8 or *ZO1*. Since maternal E-cad can mediate compaction and initiate polarization of the outside cells (Larue et al., 1994; Ohsugi et al., 1997), it was important to study the participation of N-cad in preimplantation development in the absence of maternal E-cad. After removal of maternal E-cad in the growing oocyte, E-cad expression from the paternal genome is sufficient for compaction and blastocyst formation (De Vries et al., 2004). Interestingly, under the same experimental conditions, deleting maternal E-cad but zygotically expressing N-cad from the paternal k.i. allele results in compaction and expression of epithelial markers in the outer cells. However, such embryos also fail to form an intact trophectoderm. This clearly shows that N-cad can confer cell-cell adhesion but lacks some properties needed for the formation of the trophectodermal epithelium. Thus, formation of trophectoderm in these embryos may be impaired owing to defects in the establishment of specialized cellular junctions that are required for the formation of a fully polarized epithelium (Fleming et al., 1994; Sheth et al., 2000). We noted that the tight junction protein ZO-1 is not correctly localized at the apico-lateral membrane in mutant embryos. This, together with the more extended distribution of other peripheral proteins, may indicate that N-cad is unable to assemble the cytocortical network required for proper junction formation.

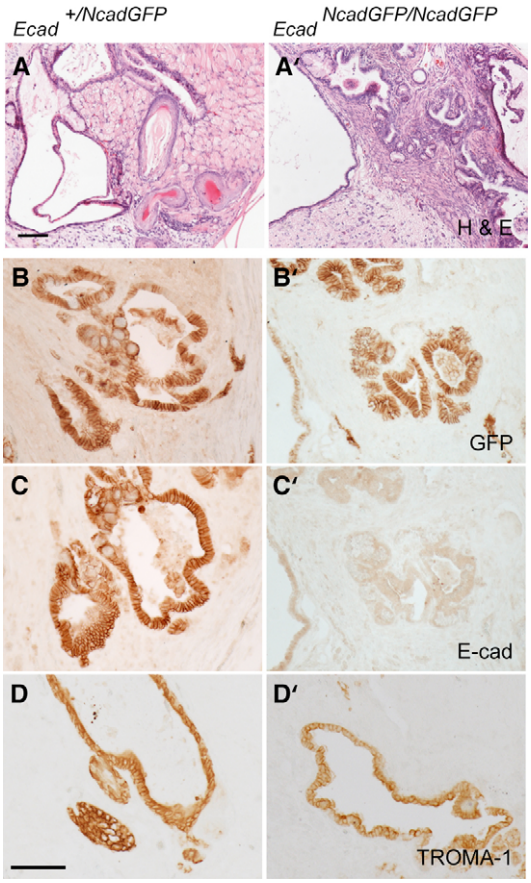

Fig. 7. ES cells derived from *Ncad-GFP* embryos can form epithelial structures in teratomas. (**A**,**A′**) Histological stainings with hematoxylin and eosin (H&E) on paraffin sections of heterozygous (A) and homozygous (A′) *Ncad-GFP* k.i. teratomas. Multiple epithelial-like structures are seen on both sections. (**B**,**B′**) Anti-GFP immunolabeling reveals expression of N-cad-GFP in epithelial cells. (**C**,**C′**) On sections consecutive to B and B′, expression of E-cad protein is detected in heterozygous teratomas (C), and is absent in homozygous *Ncad-GFP* teratomas (C′). (**D**,**D′**) Epithelia are formed in heterozygous (D) and homozygous *Ncad-GFP* teratomas (D′) and are positive for cytokeratin 8 immunolabeling. Scale bar: 100 μm.

In an earlier study, it was shown that E-cad can substitute for N-cad during cardiogenesis, suggesting that these two molecules are interchangeable in their functional properties (Luo et al., 2001). This is in contrast to our results demonstrating that N-cad cannot substitute for E-cad in early embryonic development. It may well be that N-cad cannot provide adhesive strength sufficient for the integrity of the trophectoderm epithelial cell layer. Alternatively, E-cad may be part of a trophectoderm-specific signaling program in addition to its cell adhesion program.

Attempts to overcome the developmental block of homozygous *Ncad* k.i. embryos by morula aggregation or tetraploid experiments failed, most likely owing to the segregation of E-cad- and N-cad-expressing cells from each other. However, the differentiation potential of homozygous *Ncad-GFP* ES cells could be analyzed after blastocyst injection of mutant ES cells and the generation of teratomas. We generated chimeric embryos by

injection of homozygous *Ncad* k.i. ES cells into ROSA26 blastocysts and demonstrated that both homozygous and heterozygous *Ncad* k.i. ES cells can clearly contribute to all three germ layers in vivo. They contribute to both the surface ectoderm and presumptive neural ectoderm. In the case of homozygous mutant ES cell injections, we observed strong malformations of embryos already at E7.5, which were always accompanied by a high ES cell contribution. It is likely that in embryos with a high contribution of $Ecad^{Ncad\text{-}GFP/Ncad\text{-}GFP}$ cells, normal tissue segregation is impaired. The expression of N-cad in E-cad expression domains probably perturbed the adhesive code set by the differential expression of E- and N-cad during gastrulation. In teratomas obtained with homozygous N-cad-GFP ES cells we observed various epithelial structures, such as keratinized, gland or respiratory epithelia, in the tumors that expressed N-cad. Thus, although N-cad cannot substitute for E-cad during trophectoderm differentiation, it is sufficient for epithelial formation during tumor growth. Teratomas are generated by subcutaneous injection of clumps of ES cells. The epithelial structures generated during tumor growth may be less differentiated or subject to only weak mechanical stress. By contrast, the trophectoderm is a highly specialized epithelium that must form a dense cell layer to resist the increased pressure generated by the blastocoel fluid. N-cad may not provide sufficient adhesive force to substitute for E-cad, underlining the specific requirement for E-cad for the differentiation and maintenance of the trophectodermal epithelial cell layer. It is possible that only E-cad is capable of ensuring correct assembly of the cytoskeleton and cytoskeleton-associated proteins for the cytodifferentiation processes required for a functional trophectoderm. Alternatively, E-cad may exhibit additional specific signaling functions that N-cad cannot provide.

These E-cad-specific structural and/or signaling requirements could reside in the extracellular or intracellular part of the protein. Thus, it will be of interest to analyze chimeric proteins composed of the extracellular portion of N-cad with the intracellular domain of E-cad, and vice-versa. When we designed the *Ncad* k.i. experiments, we did not anticipate such an early phenotype. We reasoned that adding N-cad to the maternal E-cad might allow early development to proceed. It remains possible that N-cad is not compatible with trophectodermal epithelial differentiation, or may even be inhibitory to this process. However, our results clearly demonstrate the specific function of E-cad during preimplantation development and provide the first in vivo evidence that E-cad and N-cad are not interchangeable in developmental processes.

The authors greatly appreciate the generous gift of antibodies from Dr P. Mangeat and Dr F. Beck. The Rat-401 anti-nestin antibody developed by Dr S. Hockfield was obtained from the Developmental Studies Hybridoma Bank, University of Iowa. We thank Davor Solter, Verdon Taylor, Michael Oelgeschlager and Ingrid Haas for helpful discussions, Randy Cassada for critical reading and Rosemary Schneider for typing of the manuscript. We thank Takashi Hiiragi and Nami Motosugi for their help with time-lapse analysis, Evelyn Wirth for technical assistance and Winfried Liebert from the MPI-IB animal facility. This work was supported by the Max-Planck Society and the German-Israeli Foundation (GIF). W.N.dV. was supported by grant number 5P20RR18789 from the National Center for Research Resources (NCRR), a component of the National Institutes of Health (NIH).

Supplementary material

Supplementary material for this article is available at http://dev.biologists.org/cgi/content/full/134/1/31/DC1

References

Aberle, H., Schwartz, H. and Kemler, R. (1996). Cadherin-catenin complex: protein interactions and their implications for cadherin function. *J. Cell Biochem.* **61**, 514-523.

Anastasiadis, P. Z. and Reynolds, A. B. (2000). The p120 catenin family: complex roles in adhesion, signaling and cancer. *J. Cell Sci.* **113**, 1319-1334.

Andreoli, C., Martin, M., Le Borgne, R., Reggio, H. and Mangeat, P. (1994). Ezrin has properties to self-associate at the plasma membrane. *J. Cell Sci.* **107**, 2509-2521.

Batlle, E., Henderson, J. T., Beghtel, H., van den Born, M. M., Sancho, E., Huls, G., Meeldijk, J., Robertson, J., van de Wetering, M., Pawson, T. et al. (2002). Beta-catenin and TCF mediate cell positioning in the intestinal epithelium by controlling the expression of EphB/ephrinB. *Cell* **111**, 251-263.

Baumgartner, W., Hinterdorfer, P., Ness, W., Raab, A., Vestweber, D., Schindler, H. and Drenckhahn, D. (2000). Cadherin interaction probed by atomic force microscopy. *Proc. Natl. Acad. Sci. USA* **97**, 4005-4010.

Beck, F., Chawengsaksophak, K., Luckett, J., Giblett, S., Tucci, J., Brown, J., Poulsom, R., Jeffery, R. and Wright, N. A. (2003). A study of regional gut endoderm potency by analysis of Cdx2 null mutant chimaeric mice. *Dev. Biol.* **255**, 399-406.

Boussadia, O., Kutsch, S., Hierholzer, A., Delmas, V. and Kemler, R. (2002). E-cadherin is a survival factor for the lactating mouse mammary gland. *Mech. Dev.* **115**, 53-62.

Braga, V. M., Del Maschio, A., Machesky, L. and Dejana, E. (1999). Regulation of cadherin function by Rho and Rac: modulation by junction maturation and cellular context. *Mol. Biol. Cell* **10**, 9-22.

Butz, S. and Larue, L. (1995). Expression of catenins during mouse embryonic development and in adult tissues. *Cell Adhes. Commun.* **3**, 337-352.

Byers, S., Amaya, E., Munro, S. and Blaschuk, O. (1992). Fibroblast growth factor receptors contain a conserved HAV region common to cadherins and influenza strain A hemagglutinins: a role in protein-protein interactions? *Dev. Biol.* **152**, 411-414.

Cepek, K. L., Shaw, S. K., Parker, C. M., Russell, G. J., Morrow, J. S., Rimm, D. L. and Brenner, M. B. (1994). Adhesion between epithelial cells and T lymphocytes mediated by E-cadherin and the alpha E beta 7 integrin. *Nature* **372**, 190-193.

Christofori, G. and Semb, H. (1999). The role of the cell-adhesion molecule E-cadherin as a tumour-suppressor gene. *Trends Biochem. Sci.* **24**, 73-76.

Chu, Y. S., Thomas, W. A., Eder, O., Pincet, F., Perez, E., Thiery, J. P. and Dufour, S. (2004). Force measurements in E-cadherin-mediated cell doublets reveal rapid adhesion strengthened by actin cytoskeleton remodeling through Rac and Cdc42. *J. Cell Biol.* **167**, 1183-1194.

Chu, Y. S., Eder, O., Thomas, W. A., Simcha, I., Pincet, F., Ben-Ze'ev, A., Perez, E., Thiery, J. P. and Dufour, S. (2006). Prototypical type I E-cadherin and type II cadherin-7 mediate very distinct adhesiveness through their extracellular domains. *J. Biol. Chem.* **281**, 2901-2910.

Corps, E., Carter, C., Karecla, P., Ahrens, T., Evans, P. and Kilshaw, P. (2001). Recognition of E-cadherin by integrin alpha(E)beta(7): requirement for cadherin dimerization and implications for cadherin and integrin function. *J. Biol. Chem.* **276**, 30862-30870.

De Vries, W. N., Evsikov, A. V., Haac, B. E., Fancher, K. S., Holbrook, A. E., Kemler, R., Solter, D. and Knowles, B. B. (2004). Maternal beta-catenin and E-cadherin in mouse development. *Development* **131**, 4435-4445.

Doetschman, T. C., Eistetter, H., Katz, M., Schmidt, W. and Kemler, R. (1985). The in vitro development of blastocyst-derived embryonic stem cell lines: formation of visceral yolk sac, blood islands and myocardium. *J. Embryol. Exp. Morphol.* **87**, 27-45.

Duguay, D., Foty, R. A. and Steinberg, M. S. (2003). Cadherin-mediated cell adhesion and tissue segregation: qualitative and quantitative determinants. *Dev. Biol.* **253**, 309-323.

Ehrlich, J. S., Hansen, M. D. and Nelson, W. J. (2002). Spatio-temporal regulation of Rac1 localization and lamellipodia dynamics during epithelial cell-cell adhesion. *Dev. Cell* **3**, 259-270.

Fedor-Chaiken, M., Hein, P. W., Stewart, J. C., Brackenbury, R. and Kinch, M. S. (2003). E-cadherin binding modulates EGF receptor activation. *Cell Commun. Adhes.* **10**, 105-118.

Fleming, T. P., Butler, L., Lei, X., Collins, J., Javed, Q., Sheth, B., Stoddart, N., Wild, A. and Hay, M. (1994). Molecular maturation of cell adhesion systems during mouse early development. *Histochemistry* **101**, 1-7.

Gumbiner, B. M. (1996). Cell adhesion: the molecular basis of tissue architecture and morphogenesis. *Cell* **84**, 345-357.

Gumbiner, B. M. (2005). Regulation of cadherin-mediated adhesion in morphogenesis. *Nat. Rev. Mol. Cell Biol.* **6**, 622-634.

Hatta, K. and Takeichi, M. (1986). Expression of N-cadherin adhesion molecules associated with early morphogenetic events in chick development. *Nature* **320**, 447-449.

Hazan, R. B. and Norton, L. (1998). The epidermal growth factor receptor modulates the interaction of E-cadherin with the actin cytoskeleton. *J. Biol. Chem.* **273**, 9078-9084.

Hazan, R. B., Phillips, G. R., Qiao, R. F., Norton, L. and Aaronson, S. A. (2000). Exogenous expression of N-cadherin in breast cancer cells induces cell migration, invasion, and metastasis. *J. Cell Biol.* **148**, 779-790.

Hazan, R. B., Qiao, R., Keren, R., Badano, I. and Suyama, K. (2004). Cadherin switch in tumor progression. *Ann. N. Y. Acad. Sci.* **1014**, 155-163.

Hiiragi, T. and Solter, D. (2004). First cleavage plane of the mouse egg is not predetermined but defined by the topology of the two apposing pronuclei. *Nature* **430**, 360-364.
Hoschuetzky, H., Aberle, H. and Kemler, R. (1994). Beta-catenin mediates the interaction of the cadherin-catenin complex with epidermal growth factor receptor. *J. Cell Biol.* **127**, 1375-1380.
Islam, S., Carey, T. E., Wolf, G. T., Wheelock, M. J. and Johnson, K. R. (1996). Expression of N-cadherin by human squamous carcinoma cells induces a scattered fibroblastic phenotype with disrupted cell-cell adhesion. *J. Cell Biol.* **135**, 1643-1654.
Kanzler, B., Haas-Assenbaum, A., Haas, I., Morawiec, L., Huber, E. and Boehm, T. (2003). Morpholino oligonucleotide-triggered knockdown reveals a role for maternal E-cadherin during early mouse development. *Mech. Dev.* **120**, 1423-1432.
Kemler, R. (1993). From cadherins to catenins: cytoplasmic protein interactions and regulation of cell adhesion. *Trends Genet.* **9**, 317-321.
Kemler, R., Babinet, C., Eisen, H. and Jacob, F. (1977). Surface antigen in early differentiation. *Proc. Natl. Acad. Sci. USA* **74**, 4449-4452.
Kemler, R., Brulet, P., Schnebelen, M. T., Gaillard, J. and Jacob, F. (1981). Reactivity of monoclonal antibodies against intermediate filament proteins during embryonic development. *J. Embryol. Exp. Morphol.* **64**, 45-60.
Koch, A. W., Manzur, K. L. and Shan, W. (2004). Structure-based models of cadherin-mediated cell adhesion: the evolution continues. *Cell Mol. Life Sci.* **61**, 1884-1895.
Kuhn, R., Rajewsky, K. and Muller, W. (1991). Generation and analysis of interleukin-4 deficient mice. *Science* **254**, 707-710.
Larue, L., Ohsugi, M., Hirchenhain, J. and Kemler, R. (1994). E-cadherin null mutant embryos fail to form a trophectoderm epithelium. *Proc. Natl. Acad. Sci. USA* **91**, 8263-8267.
Li, G. and Herlyn, M. (2000). Dynamics of intercellular communication during melanoma development. *Mol. Med. Today* **6**, 163-169.
Lickert, H., Bauer, A., Kemler, R. and Stappert, J. (2000). Casein kinase II phosphorylation of E-cadherin increases E-cadherin/beta-catenin interaction and strengthens cell-cell adhesion. *J. Biol. Chem.* **275**, 5090-5095.
Lilien, J., Balsamo, J., Arregui, C. and Xu, G. (2002). Turn-off, drop-out: functional state switching of cadherins. *Dev. Dyn.* **224**, 18-29.
Louvet, S., Aghion, J., Santa-Maria, A., Mangeat, P. and Maro, B. (1996). Ezrin becomes restricted to outer cells following asymmetrical division in the preimplantation mouse embryo. *Dev. Biol.* **177**, 568-579.
Luo, Y., Ferreira-Cornwell, M., Baldwin, H., Kostetskii, I., Lenox, J., Lieberman, M. and Radice, G. (2001). Rescuing the N-cadherin knockout by cardiac-specific expression of N- or E-cadherin. *Development* **128**, 459-469.
Miyatani, S., Shimamura, K., Hatta, M., Nagafuchi, A., Nose, A., Matsunaga, M., Hatta, K. and Takeichi, M. (1989). Neural cadherin: role in selective cell-cell adhesion. *Science* **245**, 631-635.
Niessen, C. M. and Gumbiner, B. M. (2002). Cadherin-mediated cell sorting not determined by binding or adhesion specificity. *J. Cell Biol.* **156**, 389-399.
Nollet, F., Berx, G. and van Roy, F. (1999). The role of the E-cadherin/catenin adhesion complex in the development and progression of cancer. *Mol. Cell Biol. Res. Commun.* **2**, 77-85.
Nose, A., Tsuji, K. and Takeichi, M. (1990). Localization of specificity determining sites in cadherin cell adhesion molecules. *Cell* **61**, 147-155.
Ohsugi, M., Larue, L., Schwarz, H. and Kemler, R. (1997). Cell-junctional and cytoskeletal organization in mouse blastocysts lacking E-cadherin. *Dev. Biol.* **185**, 261-271.
Ozawa, M., Baribault, H. and Kemler, R. (1989). The cytoplasmic domain of the cell adhesion molecule uvomorulin associates with three independent proteins structurally related in different species. *EMBO J.* **8**, 1711-1717.
Perret, E., Benoliel, A. M., Nassoy, P., Pierres, A., Delmas, V., Thiery, J. P., Bongrand, P. and Feracci, H. (2002). Fast dissociation kinetics between individual E-cadherin fragments revealed by flow chamber analysis. *EMBO J.* **21**, 2537-2546.
Radice, G. L., Rayburn, H., Matsunami, H., Knudsen, K. A., Takeichi, M. and Hynes, R. O. (1997). Developmental defects in mouse embryos lacking N-cadherin. *Dev. Biol.* **181**, 64-78.
Sambrook, J. and Russell, D. (1994). *Molecular Cloning: A Laboratory Manual*. Cold Spring Harbor: Cold Spring Harbor Laboratory Press.
Schwenk, F., Baron, U. and Rajewsky, K. (1995). A cre-transgenic mouse strain for the ubiquitous deletion of loxP-flanked gene segments including deletion in germ cells. *Nucleic Acids Res.* **23**, 5080-5081.
Shapiro, L., Fannon, A. M., Kwong, P. D., Thompson, A., Lehmann, M. S., Grubel, G., Legrand, J. F., Als-Nielsen, J., Colman, D. R. and Hendrickson, W. A. (1995). Structural basis of cell-cell adhesion by cadherins. *Nature* **374**, 327-337.
Sheth, B., Fontaine, J. J., Ponza, E., McCallum, A., Page, A., Citi, S., Louvard, D., Zahraoui, A. and Fleming, T. P. (2000). Differentiation of the epithelial apical junctional complex during mouse preimplantation development: a role for rab13 in the early maturation of the tight junction. *Mech. Dev.* **97**, 93-104.
Sivasankar, S., Gumbiner, B. and Leckband, D. (2001). Direct measurements of multiple adhesive alignments and unbinding trajectories between cadherin extracellular domains. *Biophys. J.* **80**, 1758-1768.
Soriano, P. (1999). Generalized lacZ expression with the ROSA26 Cre reporter strain. *Nat. Genet.* **21**, 70-71.
Stemmler, M. P., Hecht, A., Kinzel, B. and Kemler, R. (2003). Analysis of regulatory elements of E-cadherin with reporter gene constructs in transgenic mouse embryos. *Dev. Dyn.* **227**, 238-245.
Stemmler, M. P., Hecht, A. and Kemler, R. (2005). E-cadherin intron 2 contains cis-regulatory elements essential for gene expression. *Development* **132**, 965-976.
Suyama, K., Shapiro, I., Guttman, M. and Hazan, R. B. (2002). A signaling pathway leading to metastasis is controlled by N-cadherin and the FGF receptor. *Cancer Cell* **2**, 301-314.
Takeichi, M. (1988). The cadherins: cell-cell adhesion molecules controlling animal morphogenesis. *Development* **102**, 639-655.
Tomita, K., van Bokhoven, A., van Leenders, G. J., Ruijter, E. T., Jansen, C. F., Bussemakers, M. J. and Schalken, J. A. (2000). Cadherin switching in human prostate cancer progression. *Cancer Res.* **60**, 3650-3654.
Vestweber, D. and Kemler, R. (1984). Rabbit antiserum against a purified surface glycoprotein decompacts mouse preimplantation embryos and reacts with specific adult tissues. *Exp. Cell Res.* **152**, 169-178.
Wilkinson, D. and Green, J. (1990). In situ hybridization and three-dimensional reconstruction of serial sections. In *Postimplantation Mouse Embryos: A Practical Approach* (ed. D. Rickwood and D. L. Cockcroft), pp. 155-171. Oxford: IRL Press.
Williams, E. J., Furness, J., Walsh, F. S. and Doherty, P. (1994). Activation of the FGF receptor underlies neurite outgrowth stimulated by L1, N-CAM, and N-cadherin. *Neuron* **13**, 583-594.